SC-FDMA for Multiuser Communication on the Downlink

Harsha S. Eshwaraiah and A. Chockalingam
Department of ECE, Indian Institute of Science, Bangalore

***Abstract*—Single-carrier frequency division multiple access (SC-FDMA) has become a popular alternative to orthogonal frequency division multiple access (OFDMA) in multiuser communication on the uplink. This is mainly due to the low peak-to-average power ratio (PAPR) of SC-FDMA compared to that of OFDMA. Long-term evolution (LTE) uses SC-FDMA on the uplink to exploit this PAPR advantage to reduce transmit power amplifier backoff in user terminals. In this paper, we show that SC-FDMA can be beneficially used for multiuser communication on the downlink as well. We present SC-FDMA transmit and receive signaling architectures for multiuser communication on the downlink. The benefits of using SC-FDMA on the downlink are that SC-FDMA can achieve i) significantly better bit error rate (BER) performance at the user terminal compared to OFDMA, and ii) improved PAPR compared to OFDMA which reduces base station (BS) power amplifier backoff (making BSs more green). SC-FDMA receiver needs to do joint equalization, which can be carried out using low complexity equalization techniques. For this, we present a local neighborhood search based equalization algorithm for SC-FDMA. This algorithm is very attractive both in complexity as well as performance. We present simulation results that establish the PAPR and BER performance advantage of SC-FDMA over OFDMA in multiuser SISO/MIMO downlink as well as in large-scale multiuser MISO downlink with tens to hundreds of antennas at the BS.**

Keywords *– Multiuser downlink, SISO/MIMO ISI channels, SC-FDMA, OFDMA, PAPR, frequency domain equalization.*

I. Introduction

Transmission rates on wireless channels are on the increase to meet the increasing data rate requirements posed by the growing wireless data traffic. Increased transmission rates render the wireless channel more and more frequency selective. Inter-symbol interference (ISI) caused due to the presence of several delayed multipath components in such channels is a concern. Multicarrier signaling techniques are popularly used on ISI channels [1]. Orthogonal frequency division multiplexing (OFDM) is one such multicarrier technique. By using several subcarriers of narrow bandwidth instead of a single carrier of a larger bandwidth, OFDM signaling attempts to make individual subcarriers see frequency-flat fading, which, in turn, can allow simple one-tap equalization at the receiver. OFDM has been widely adopted in several wireless systems and standards, e.g., IEEE 802.11a/g/n.

In the context of multiuser communication, orthogonal frequency division multiple access (OFDMA) presents the benefits of flexible resource allocation (subcarrier allocation to users) and scheduling. Dynamic allocation of subcarriers in OFDMA can further improve performance compared to fixed allocation. Because of these advantages, OFDMA has been adopted in wireless standards including WiMax and LTE.

978-1-4673-5494-3/13/$31.00

However, a drawback with OFDMA is the large peak-to-average power ratio (PAPR) in OFDM modulated signals. This necessitates the transmitter RF power amplifiers (PA) to work with large backoffs (i.e., transmitter PAs are made to operate at low efficiency operating points to ensure linearity). Because of this power inefficiency due to the PAPR issue, and since mobiles/user terminals are more power constrained than base stations, LTE uses OFDMA only on the downlink and not on the uplink.

Single-carrier signals, on the other hand, have much lower PAPR [2]- [4]. To exploit this benefit, LTE uses single-carrier frequency division multiple access (SC-FDMA) on the uplink [5], [6]. Although SC-FDMA is a single-carrier technique, in terms of implementation, it can be viewed as a DFT-precoded OFDM (i.e., DFT operation preceding the IDFT operation in OFDM). In addition to the PAPR advantage, the DFT precoded OFDM view of SC-FDMA allows it to retain the flexible resource allocation advantage of OFDMA as well.

In this paper, we argue and show that SC-FDMA can be used beneficially on the downlink as well. A key advantage is that base station operation can be made more energy efficient. With the growing need to design energy efficient 'green' base stations, the choice of single-carrier communication for the downlink is in the right direction. While SC-FDMA allows the base station power amplifiers to work at more efficient operating points because of its low PAPR, it can also offer the additional benefit of performing significantly better than OFDMA. We first present SC-FDMA transmit and receive signaling architectures for multiuser communication on the downlink. We consider SC-FDMA in both multiuser SISO as well as multiuser MIMO downlink. We also consider the emerging area of large-scale MIMO, where the base station has tens to hundreds of antennas and the user terminals have much fewer number of antennas (e.g., one antenna).

A key requirement in SC-FDMA is the need to do joint equalization at the receiver. While this will imply increased receiver complexity than in OFDMA, several low-complexity algorithms reported in the recent literature show good promise for use in SC-FDMA equalization. In particular, these algorithms are of the same order of complexity as linear receivers like ZF and MMSE, and they achieve close to optimal performance in large dimensions. We use one such low complexity algorithm based on local neighborhood search, namely, likelihood ascent search (LAS) algorithm [7], [8], for equalization of SC-FDMA signals at the user terminal. Our simulation results establish the PAPR and BER performance advantage of SC-FDMA over OFDMA in multiuser SISO/MIMO downlink as well as in large-scale multiuser MISO downlink with tens to hundreds of antennas at the BS. This performance advantage

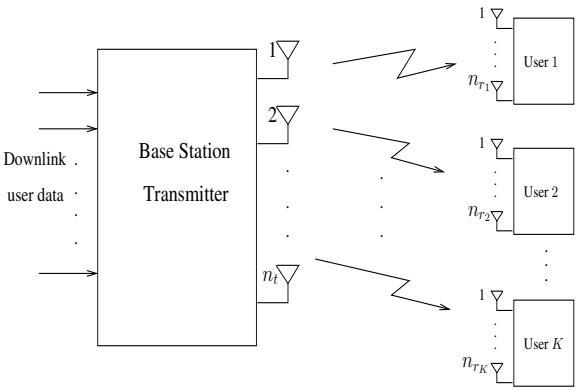

Fig. 1. Multiuser MIMO downlink system.

coupled with low PAPR advantage makes SC-FDMA a preferred choice for multiuser downlink communication in future wireless systems and standards.

The rest of this paper is organized as follows. The multiuser SC-FDMA system on the downlink, including the transmit and receive chains, frequency-domain equalization/detection algorithm, and subcarrier allocation algorithms are presented in Section II. Simulation results on the PAPR and BER performance of SC-FDMA on the downlink in comparison with those of OFDMA are presented in Section III. Conclusions are given in Section IV.

Notation: Vectors and matrices are denoted by bold face lowercase and bold face uppercase letters, respectively. $[.]^T$, $(.)^H$, $(.)^\dagger$ denote transpose, Hermitian, and pseudo inverse, respectively. $\|.\|_F$, $\|.\|_2$ denote frobenius norm and euclidean norm, respectively. $|.|$ denotes cardinality of a set and $\emptyset$ denotes the empty set. $\mathbf{F}_P$ and $\tilde{\mathbf{F}}_P$ denote P-point DFT and IDFT matrices, respectively.

II. Multiuser SC-FDMA on the Downlink

Consider a multiuser downlink system with n_t transmit antennas at the base station and K downlink users, each having one or more receive antennas, as shown in Fig. 1. Without loss of generality let us that assume all users have n_r receive antennas each, and that $Q \triangleq \min(n_t, n_r)$ denote the maximum number of data streams for each user. The channel between each transmit-receive antenna pair is assumed to be frequency selective with L taps. Let $h_{i,j}^u(l), l = 0, 1, \cdots, L-1$ be the lth time domain channel coefficient between the ith transmit antenna and jth receive antenna of the uth user, $i = 1, \cdots, n_t$, $u = 1, \cdots, K$, $j = 1, \cdots, n_r$.

Let N denote the number of subcarriers in the system. The subcarriers can be allotted to the users on a fixed or dynamic basis (e.g., based on channel state information). Let each subcarrier be used by a maximum of $\widetilde{K}$ users simultaneously, where $\widetilde{K}$ is defined as

$$\widetilde{K} \triangleq \begin{cases} \min(\lfloor \frac{n_t}{n_r} \rfloor, K), & n_t > n_r \\ 1, & \text{otherwise.} \end{cases} \quad (1)$$

In other words, each user is allocated $M \triangleq \lfloor \frac{N\widetilde{K}}{K} \rfloor$ subcarriers. We assume equal power allocation and bit loading on all subcarriers.

The detailed block diagrams of the base station transmitter and the uth user's receiver are shown in the Fig. 2. Let $\mathbb{S}_n = \{1_n, 2_n, \cdots, \widetilde{K}_n\}$ denote the set of users sharing subcarrier n, and $\mathbb{A}_u = \{1_u, 2_u, \cdots, M_u\}$ denote the set of subcarriers allocated to user u. Let $\mathbf{x}^u$ denote the information data block of length MQ for user u. The output of the M-point DFT block (Fig. 2) is given by

$$\tilde{\mathbf{x}}_j^u = \mathbf{F}_M \mathbf{x}_j^u, \quad j = 1, 2, \cdots, Q, \quad (2)$$

where $\mathbf{F}_M$ is the M-point DFT matrix, $\mathbf{x}_j^u = [x^u((j-1)M+1), x^u((j-1)M+2), \cdots, x^u((j-1)M+M)]^T$, and $x^u(m)$ is the mth data symbol of the uth user. The output vectors from the DFT blocks are given to the beamforming and subcarrier allocation block. Let $\mathbf{P}_n^u$ denote the $n_t \times Q$ beamforming/precoding matrix for user u on subcarrier n. We use SVD precoding [9], [12] to eliminate other-user interference. The precoded output vector of size $n_t \times 1$ for user u on subcarrier n is then given by

$$\tilde{\mathbf{z}}^u(n) = \mathbf{P}_n^u \tilde{\mathbf{x}}^u(n), \quad n = 1_u, 2_u, \cdots, M_u, \quad (3)$$

where $\tilde{\mathbf{x}}^u(n) = [\tilde{x}_1^u(n), \tilde{x}_2^u(n), \cdots, \tilde{x}_Q^u(n)]^T$, $n = 1_u, \cdots, M_u$, and $\tilde{x}_j^u(n)$ is the nth element of $\tilde{\mathbf{x}}_j^u$. Let $\mathbf{A}^k$ denote the $N \times M$ subcarrier allocation matrix for user k, $k = 1, \cdots, K$. An example of subcarrier allocation algorithm to get $\mathbf{A}^k$, $k = 1, \cdots, K$ is given in Section II-B. The $N \times 1$ vector input to the N-point IDFT block on the ith transmit chain is given by

$$\mathbf{d}_i = \sum_{k=1}^{K} \mathbf{A}^k \tilde{\mathbf{z}}_i^k, \quad i = 1, 2, \cdots, n_t, \quad (4)$$

where $\tilde{\mathbf{z}}_i^u = [\tilde{z}_i^u(1_u), \tilde{z}_i^u(2_u), \cdots, \tilde{z}_i^u(M_u)]^T$, $i = 1, \cdots, n_t$. The output of N-point IDFT block on the ith transmit chain is given by

$$\mathbf{s}_i = \tilde{\mathbf{F}}_N \mathbf{d}_i, \quad i = 1, 2, \cdots, n_t, \quad (5)$$

where $\tilde{\mathbf{F}}_N$ denotes the N-point IDFT matrix. The transmit signal vector $\mathbf{s}_i$ is transmitted on antenna i after addition of cyclic prefix (CP) of length $L-1$. Note that the above SC-FDMA transmitter (in Fig. 2) becomes OFDMA transmitter if the M-point DFT blocks are removed.

Now, the received signal vector of size $N \times 1$ at the uth user on the jth receive antenna, after removing the CP, is given by

$$\mathbf{y}_j^u = \sum_{i=1}^{n_t} \mathbf{h}_{i,j}^u \circledast \mathbf{s}_i + \mathbf{q}_j^u, \quad j = 1, 2, \cdots, n_r, \quad (6)$$

where $\circledast$ denotes N-point circular convolution operation, $\mathbf{h}_{i,j}^u = [h_{i,j}^u(0), h_{i,j}^u(1), \cdots, h_{i,j}^u(L-1), \ (N-L) \text{ zeros}]^T$, and $\mathbf{q}_j^u \in \mathcal{CN}(0, N_0 \mathbf{I}_N)$ is the additive noise vector. The output signal is then converted to frequency domain by taking N-

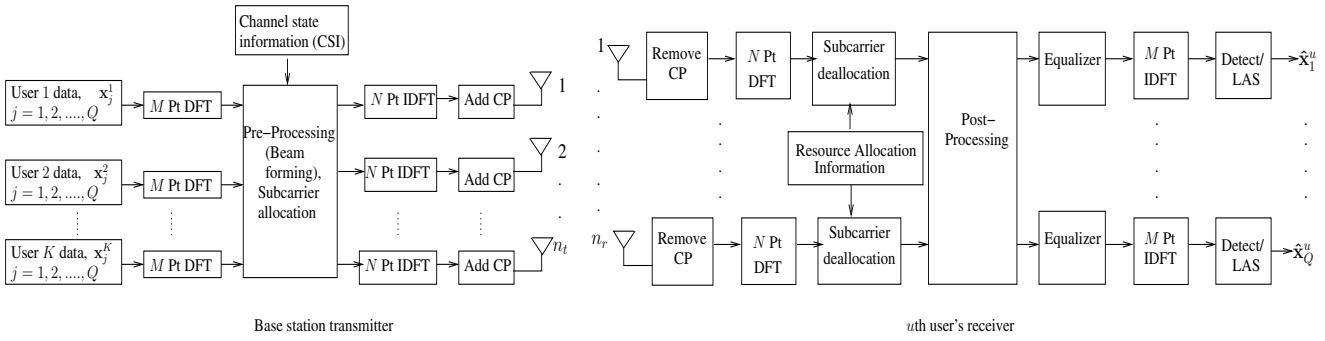

Fig. 2. Transmitter and receiver block diagrams of MIMO SC-FDMA on the downlink.

point DFT, which is given by

$$\begin{aligned}\tilde{\mathbf{y}}_j^u &= \mathbf{F}_N \mathbf{y}_j^u, \quad j = 1, 2, \cdots, n_r \\ \tilde{\mathbf{y}}_j^u &= \sum_{i=1}^{n_t} \mathbf{H}_{i,j}^u \mathbf{d}_i + \tilde{\mathbf{q}}_j^u, \\ &= \sum_{i=1}^{n_t} \mathbf{H}_{i,j}^u \sum_{k=1}^{K} \mathbf{A}^k \tilde{\mathbf{z}}_i^k + \tilde{\mathbf{q}}_j^u, \end{aligned} \tag{7}$$

where $\mathbf{H}_{i,j}^u = \text{diag}(\mathbf{F}_N \mathbf{h}_{i,j}^u)$ is the $N \times N$ diagonal matrix whose diagonal elements are the frequency domain channel coefficients between ith transmit antenna and jth receive antenna of user u. Now, $\tilde{\mathbf{y}}_j^u$ is applied to the subcarrier deallocation block to get

$$\begin{aligned}\bar{\mathbf{y}}_j^u &= \tilde{\mathbf{A}}^u \tilde{\mathbf{y}}_j^u, \quad j = 1, 2, \cdots, n_r \\ &= \sum_{i=1}^{n_t} \sum_{k=1}^{K} \tilde{\mathbf{A}}^u \mathbf{H}_{i,j}^u \mathbf{A}^k \tilde{\mathbf{z}}_i^k + \underbrace{\tilde{\mathbf{A}}^u \tilde{\mathbf{q}}_j^u}_{\bar{\mathbf{q}}_j^u}, \end{aligned} \tag{8}$$

where $\tilde{\mathbf{A}}^u$ is the deallocation matrix for the uth user, given by $\tilde{\mathbf{A}}^u = (\mathbf{A}^u)^T$. Simplifying the above equation, we get

$$\bar{\mathbf{y}}^u(n) = \mathbf{H}^u(n) \sum_{k \in \mathbb{S}_n} \mathbf{P}_n^k \tilde{\mathbf{x}}^k(n) + \bar{\mathbf{q}}^u(n), \quad u \in \mathbb{S}_n, \tag{9}$$

where $\bar{\mathbf{y}}^u(n) = [\tilde{y}_1^u(n), \tilde{y}_2^u(n), \cdots, \tilde{y}_{n_r}^u(n)]^T$, $\tilde{y}_j^u(n)$ is the nth element of $\tilde{\mathbf{y}}_j^u$, $\mathbf{H}^u(n)$ is $n_r \times n_t$ frequency domain channel coefficient matrix of user u on subcarrier n, whose (l,k)th entry is the nth diagonal element of the matrix $\mathbf{H}_{k,l}^u$, and $\bar{\mathbf{q}}^u(n) = [\tilde{q}_1^u(n), \tilde{q}_2^u(n), \cdots, \tilde{q}_{n_r}^u(n)]^T$, where $\tilde{q}_j^u(n)$ is the nth element of $\tilde{\mathbf{q}}_j^u$.

As mentioned earlier, we use SVD to get the beamforming/precoding matrices at the transmitter. The SVD decomposition of channel matrix $\mathbf{H}^u(n)$ is given by

$$\mathbf{H}^u(n) = \mathbf{U}_n^u \mathbf{\Sigma}_n^u (\mathbf{V}_n^u)^H, \tag{10}$$

where $\mathbf{U}_n^u$ is a matrix of size $n_r \times Q$ containing the left singular vectors, $\mathbf{\Sigma}_n^u$ is a diagonal matrix of size $Q \times Q$ containing singular values, and $(\mathbf{V}_n^u)$ is a matrix of size $n_t \times Q$ containing the right singular vectors. Let us define the following vectors and matrices:

$$\tilde{\mathbf{x}}(n) \triangleq [(\tilde{\mathbf{x}}^{1_n}(n))^T, (\tilde{\mathbf{x}}^{2_n}(n))^T, \cdots, (\tilde{\mathbf{x}}^{\tilde{K}_n}(n))^T]^T,$$

$$\mathbf{P}_n \triangleq [\mathbf{P}_n^{1_n}, \mathbf{P}_n^{2_n}, \cdots, \mathbf{P}_n^{\tilde{K}_n}],$$

$$\mathbf{U}_n \triangleq \text{diag}(\mathbf{U}_n^{1_n}, \mathbf{U}_n^{2_n}, \cdots, \mathbf{U}_n^{\tilde{K}_n}),$$

$$\mathbf{\Sigma}_n \triangleq \text{diag}(\mathbf{\Sigma}_n^{1_n}, \mathbf{\Sigma}_n^{2_n}, \cdots, \mathbf{\Sigma}_n^{\tilde{K}_n}),$$

$$\mathbf{V}_n \triangleq [\mathbf{V}_n^{1_n}, \mathbf{V}_n^{2_n}, \cdots, \mathbf{V}_n^{\tilde{K}_n})],$$

$$\bar{\mathbf{q}}(n) \triangleq [(\bar{\mathbf{q}}^{1_n}(n))^T, (\bar{\mathbf{q}}^{2_n}(n))^T, \cdots, (\bar{\mathbf{q}}^{\tilde{K}_n}(n))^T]^T,$$

$$\bar{\mathbf{y}}(n) \triangleq [(\bar{\mathbf{y}}^{1_n}(n))^T, (\bar{\mathbf{y}}^{2_n}(n))^T, \cdots, (\bar{\mathbf{y}}^{\tilde{K}_n}(n))^T]^T.$$

The received signal vector on subcarrier n due to all the users sharing it can be written as

$$\bar{\mathbf{y}}(n) = \mathbf{U}_n \mathbf{\Sigma}_n (\mathbf{V}_n)^H \mathbf{P}_n \tilde{\mathbf{x}}(n) + \bar{\mathbf{q}}(n). \tag{11}$$

The multiuser interference can be completely eliminated by choosing the beamforming/precoder matrix as

$$\mathbf{P}_n = \alpha_n [(\mathbf{V}_n)^H]^\dagger \quad \text{s. t. } \mathbb{E}[\|\mathbf{P}_n \tilde{\mathbf{x}}(n)\|_2^2] = \rho, \tag{12}$$

where α_n is the power normalization factor. Equation (11) can be written as

$$\bar{\mathbf{y}}(n) = \alpha_n \mathbf{U}_n \mathbf{\Sigma}_n \tilde{\mathbf{x}}(n) + \bar{\mathbf{q}}(n). \tag{13}$$

Now, the received signal vector on subcarrier n at user u sharing it is given by

$$\bar{\mathbf{y}}^u(n) = \mathbf{U}_n^u \tilde{\mathbf{\Sigma}}_n^u \tilde{\mathbf{x}}^u(n) + \bar{\mathbf{q}}^u(n), \quad u \in \mathbb{S}_n, \tag{14}$$

where $\tilde{\mathbf{\Sigma}}_n^u = \alpha_n \mathbf{\Sigma}_n^u$.

The receiver signal processing at user u is done as follows. First, doing post-processing operation on the received signal vector $\bar{\mathbf{y}}^u(n)$ by multiplying with $(\mathbf{U}_n^u)^H$, we get

$$\begin{aligned}\hat{\mathbf{y}}^u(n) &= (\mathbf{U}_n^u)^H \bar{\mathbf{y}}^u(n) \\ &= \tilde{\mathbf{\Sigma}}_n^u \tilde{\mathbf{x}}^u(n) + \mathbf{w}^u(n). \end{aligned} \tag{15}$$

Define the following vectors and matrices:

$$\hat{\mathbf{y}}_j^u = [\hat{y}_j^u(1_u), \hat{y}_j^u(2_u), \cdots, \hat{y}_j^u(M_u)]^T,$$

$$\tilde{\mathbf{\Sigma}}^u(j) = \text{diag}(\tilde{\Sigma}_{1_u}^u(j,j), \tilde{\Sigma}_{2_u}^u(j,j), \cdots, \tilde{\Sigma}_{M_u}^u(j,j)),$$

$$\tilde{\mathbf{x}}_j^u = [\tilde{x}_j^u(1_u), \tilde{x}_j^u(2_u), \cdots, \tilde{x}_j^u(M_u)]^T,$$

$$\tilde{\mathbf{w}}_j^u = [\tilde{w}_j^u(1_u), \tilde{w}_j^u(2_u), \cdots, \tilde{w}_j^u(M_u)]^T,$$

where $\tilde{\Sigma}_n^u(j,j)$ is the jth diagonal element of $\tilde{\mathbf{\Sigma}}_n^u$. Using the above definitions, the signal vector at user u on stream j and allocated subcarrier set $\mathbb{A}_u$ can be written as

$$\hat{\mathbf{y}}_j^u = \tilde{\mathbf{\Sigma}}^u(j)\tilde{\mathbf{x}}_j^u + \mathbf{w}_j^u, \quad j = 1, 2, \cdots, Q. \tag{16}$$

On the received signal model in (16), we carry out frequency domain equalization and detection on a per-stream basis at the user terminal.

A. Low-complexity frequency-domain equalization/detection

In this subsection, we present the equalization and detection scheme for the jth stream at the uth user. We propose to use a frequency-domain MMSE (FD-MMSE) equalizer followed by a likelihood ascent search (LAS) algorithm [7], [8], which is a local neighborhood search algorithm, to carry out equalization and detection. The FD-MMSE equalization operation for the jth stream at user u is given by

$$\hat{\tilde{\mathbf{x}}}_j^u = \left((\tilde{\Sigma}_j^u)^H(\tilde{\Sigma}_j^u) + (N_0/E_s)\mathbf{I}_M\right)^{-1}(\tilde{\Sigma}_j^u)^H\tilde{\mathbf{y}}_j^u. \tag{17}$$

The FD-MMSE equalizer output vector in (17) is converted to time domain by an M-point IDFT operation, followed by detection. Though the FD-MMSE equalizer is attractive because of its low complexity, its performance is far from the optimum performance. Therefore, in order to improve performance, we employ the LAS algorithm at the output of the FD-MMSE equalizer. Starting from the FD-MMSE equalizer output symbol vector, the LAS algorithm reaches a locally optimum solution through a low-complexity local neighborhood search. The LAS algorithm works as follows. Equation (16) can be written as

$$\hat{\mathbf{y}}_j^u = \underbrace{\tilde{\mathbf{\Sigma}}^u(j)\mathbf{F}_M}_{\mathbf{G}^u(j)}\mathbf{x}_j^u + \mathbf{w}_j^u, \quad j = 1, 2, \cdots, Q. \tag{18}$$

Writing (18) in real form and leaving indices for simplicity, we have

$$\mathbf{y} = \mathbf{G}\mathbf{x} + \mathbf{w}, \tag{19}$$

where $\mathbf{y} = [\Re(\hat{\mathbf{y}}_j^u)^T \ \Im(\hat{\mathbf{y}}_j^u)^T]^T$, $\mathbf{x} = [\Re(\mathbf{x}_j^u)^T \ \Im(\mathbf{x}_j^u)^T]^T$, $\mathbf{w} = [\Re(\mathbf{w}_j^u)^T \ \Im(\mathbf{w}_j^u)^T]^T$, $\mathbf{G} = \begin{bmatrix} \Re(\mathbf{G}_j^u) & \Im(\mathbf{G}_j^u) \\ \Re(\mathbf{G}_j^u) & \Im(\mathbf{G}_j^u) \end{bmatrix}$, and $\Re(.)$ and $\Im(.)$ denote the real and imaginary parts, respectively. In this real-valued system model, the maximum likelihood (ML) cost can be written as

$$\psi(\mathbf{x}) = \|\mathbf{y} - \mathbf{G}\mathbf{x}\|^2 = \mathbf{x}^T\mathbf{G}^T\mathbf{G}\mathbf{x} - 2\mathbf{x}^T\mathbf{G}^T\mathbf{y}. \tag{20}$$

The LAS algorithm starts with an initial solution vector $\mathbf{x}^{(0)}$. The output symbol vector from the FD-MMSE equalizer is used as the initial solution vector. A neighborhood around the initial vector is defined to be the set of all vectors which differ from the initial vector in one coordinate. For each of the vectors in the neighborhood, the algorithm computes the ML cost function $\psi(\mathbf{x})$ defined in (20). The best vector among the neighboring vectors (in terms of least ML cost among them) which also happens to have a lesser ML cost than that of the initial vector is chosen, and declared as the new solution vector $\mathbf{x}^{(1)}$; the 1 in the superscript denotes the iteration index. This new solution vector $\mathbf{x}^{(1)}$ is passed on as the initial vector for the next iteration, where the best vector among the neighboring vectors of $\mathbf{x}^{(1)}$ is chosen as the new solution vector for the next iteration, and so on until a local minima is reached. The algorithm ends once a local minima is encountered. The solution vector corresponding to the local minima is declared as the final solution vector.

B. Subcarrier allocation

In this subsection, we present the subcarrier allocation algorithms used at the transmitter for two cases, namely, $\widetilde{K} = 1$ and $\widetilde{K} > 1$. The algorithm for $\widetilde{K} = 1$ (**Algorithm 1**) is from [10]. The algorithm for $\widetilde{K} > 1$ (**Algorithm 2**) is from [11]. These algorithms were proposed for subcarrier allocation in OFDMA downlink. Therefore, using the same algorithms for subcarrier allocation in SC-FDMA allows us to compare the performance of OFDMA and SC-FDMA under similar system settings.

1) Subcarrier allocation algorithm for $\widetilde{K} = 1$: In this case, each subcarrier is allotted to only one user, and each user will get N/K subcarriers. The subcarrier allocation algorithm for this case is from [10], which is presented in **Algorithm 1** below.

Algorithm 1 Subcarrier allocation algorithm for $\widetilde{K} = 1$

$\mathbb{U} = \{1, 2, \cdots, K\}$, $\mathbb{B} = \{1, 2, \cdots, N\}$
Initialize: $\mathbb{S}_n = \emptyset, \forall\, n \in \mathbb{B}$; $\mathbb{A}_u = \emptyset, \forall\, u \in \mathbb{U}$
while $|\mathbb{B}| > 0$ **do**
  for each $n \in \mathbb{B}$ **do**
    Find the frobenius norm of the channel coefficient matrix over subcarrier n, for all the users in $\mathbb{U}$.
    Arrange the users in $\mathbb{U}$ in descending order based on the frobenius norm values.
    Calculate the difference D_n between the frobenius norm value of first best user and frobenius norm value of second best user.
  end for
  $n' = \underset{n}{\operatorname{argmax}}\, D_n$
  Find user u' with maximum frobenius norm value in subcarrier n'.
  if $|\mathbb{A}_{u'}| < M$ **then**
    $\mathbb{A}_{u'} = \mathbb{A}_{u'} \cup n'$; $\mathbb{B} = \mathbb{B} - n'$; $\mathbb{S}_{n'} = \mathbb{S}_{n'} \cup u'$
  else
    $\mathbb{U} = \mathbb{U} - u'$
  end if
end while

2) Subcarrier allocation algorithm for $\widetilde{K} > 1$: In this case, each subcarrier can be allotted to a maximum of $\widetilde{K}$ users. We use a correlation based algorithm from [11] for subcarrier allocation in this case. The algorithm is presented in **Algorithm 2** below.

Algorithm 2 Subcarrier allocation algorithm for $\widetilde{K} > 1$

The channel correlation metric between user i and user j is calculated over each subcarrier n as:

$$\eta_{i,j}^{n} = \frac{\|\mathbf{H}_i^n \mathbf{H}_j^n\|_F^2}{\|\mathbf{H}_i^n\|_F^2 \|\mathbf{H}_j^n\|_F^2}$$

$\mathbb{B} = \{1, 2, \cdots, N\}$; $\mathbb{U}_n = \{1, 2, \cdots, K\}, \forall\, n \in \mathbb{B}$
Initialize: $\mathbb{S}_n = \emptyset, \forall\, n \in \mathbb{B}$; $\mathbb{A}_u = \emptyset, \forall\, u \in \mathbb{U}_n$
for each $n \in \mathbb{B}$ **do**
  Find $u = \underset{k \in \mathbb{U}_n, |\mathbb{A}_k| < M}{\operatorname{argmax}} \|\mathbf{H}_n^u\|_F^2$
  $\mathbb{S}_n = \mathbb{S}_n \cup u$; $\mathbb{U}_n = \mathbb{U}_n - u$; $\mathbb{A}_u = \mathbb{A}_u \cup n$
  while $|\mathbb{S}_n| < \tilde{K}$ **do**
    $\hat{u} = \underset{k \in \mathbb{U}_n, |\mathbb{A}_k| < M}{\operatorname{argmin}} \sum_{m \in \mathbb{S}_n} \eta_{m,k}^{n}$
    if no $\hat{u}$ found **then**
      Break the loop
    else
      $\mathbb{U}_n = \mathbb{U}_n - \hat{u}$; $\mathbb{A}_{\hat{u}} = \mathbb{A}_{\hat{u}} \cup n$; $\mathbb{S}_n = \mathbb{S}_n \cup \hat{u}$
    end if
  end while
end for

III. Results and Discussion

In this section, we present the PAPR and BER performance results of SC-FDMA on the downlink obtained through simulations. We compare the performance of SC-FDMA and OFDMA for the same system settings. In all the simulations, we have taken the channel between each transmit and receive antenna for all users to be frequency selective with $L = 5$ taps and uniform power delay profile (UPDP). For subcarrier allocation, two methods are considered: i) fixed interleaved allocation, and ii) dynamic allocation. Fixed interleaved allocation is a static method of allocation in which subcarriers are allocated in an interleaved fashion [5]. For example, in a SISO system with N subcarriers and K users, each user is allotted with $M = N/K$ subcarriers such that user k is allotted the subcarriers $n = k + (i-1)K$, $i = 1, 2, \cdots, M$. In dynamic allocation, subcarriers are allocated based on channel state information (CSI) using either of the two algorithms, namely, **Algorithm 1** and **Algorithm 2** in Section II-B, depending on the value of $\widetilde{K}$. We assume perfect knowledge of the CSI. We use 4-QAM in the BER simulations, and 16-QAM in the PAPR simulations. In SC-FDMA, we use FD-MMSE equalizer followed by LAS algorithm (referred to as FD-MMSE LAS). In OFDMA, we use a single-tap equalizer followed by detection.

A. PAPR and BER of multiuser SISO SC-FDMA downlink

In a SISO multiuser downlink system, $n_t = n_r = 1$. Therefore, $\widetilde{K} = 1$ and **Algorithm 1** is used for dynamic subcarrier allocation. In Fig. 3, we show the PAPR performance of SC-FDMA and OFDMA for $n_t = 1, n_r = 1, K = 4, N = 128$, 16-QAM, and fixed interleaved allocation of subcarriers. It can be seen that SC-FDMA has significantly better PAPR than OFDMA. For the same system parameters, Fig. 4 shows the BER performance of SC-FDMA and OFDMA for 4-QAM and dynamic subcarrier allocation. SC-FDMA BER plots with i) FD-MMSE equalizer only, and ii) FD-MMSE equalizer followed by LAS algorithm are shown. From Fig. 4, we observe that i) SC-FDMA achieves better BER performance than that of OFDMA, and ii) using the LAS algorithm at the output of FD-MMSE equalizer improves the BER performance of the FD-MMSE equalizer.

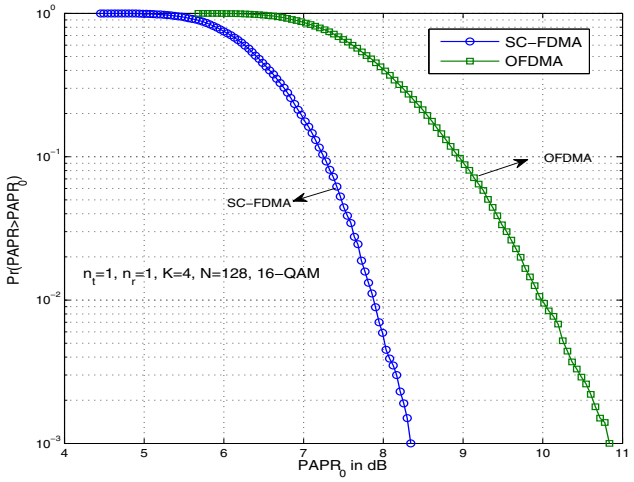

Fig. 3. PAPR performance of multiuser SISO SC-FDMA and OFDMA for $n_t = 1, n_r = 1, K = 4, N = 128$, 16-QAM.

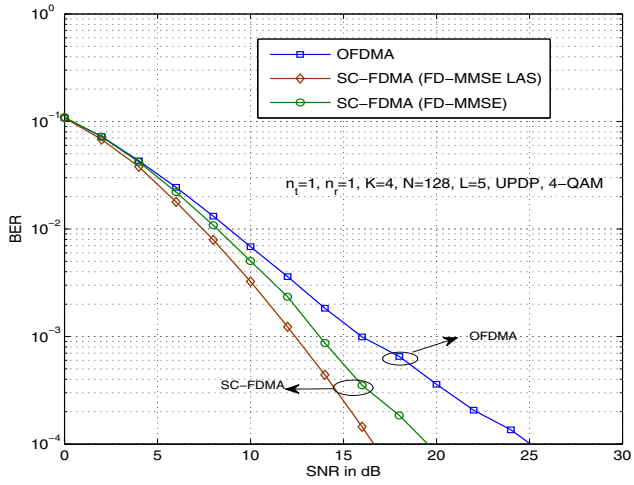

Fig. 4. BER performance of multiuser SISO downlink SC-FDMA and OFDMA for $n_t = 1, n_r = 1, K = 4, N = 128, L = 5$, 4-QAM.

B. PAPR and BER of multiuser MIMO SC-FDMA downlink

Here, we present the PAPR and BER results for multiuser MIMO SC-FDMA and OFDMA systems with $n_t = 4, n_r = 2, K = 4, N = 64$. In this case, $\widetilde{K} = 2$, and each subcarrier is

shared by two users. **Algorithm 2** is used for dynamic subcarrier allocation. Figure 5 shows the PAPR comparison between SC-FDMA and OFDMA for 16-QAM and fixed interleaved subcarrier allocation. Figure 6 shows the BER comparison between SC-FDMA and OFDMA under both fixed allocation and dynamic allocation. We observe that SC-FDMA exhibits significantly better PAPR and BER performance compared to OFDMA in multiuser MIMO downlink scenario also.

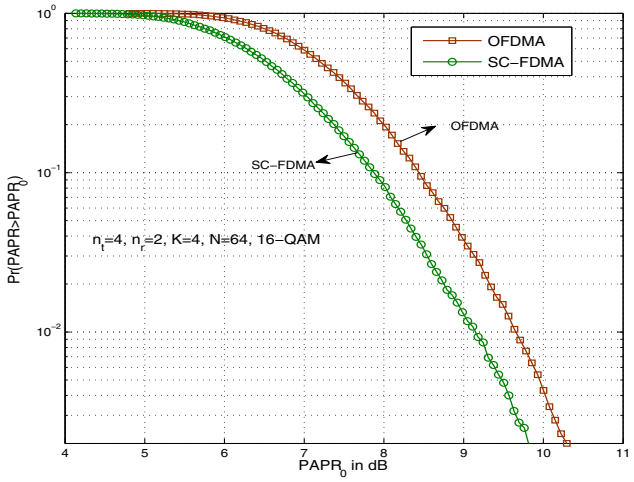

Fig. 5. PAPR performance of multiuser MIMO SC-FDMA and OFDMA for $n_t = 4, n_r = 2, K = 4, N = 64$, 16-QAM.

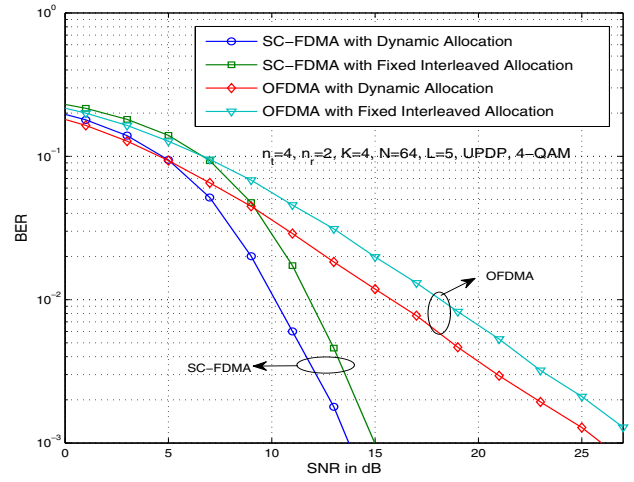

Fig. 6. BER performance of multiuser MIMO downlink SC-FDMA and OFDMA for $n_t = 4, n_r = 2, K = 4, N = 64, L = 5$, 4-QAM.

C. PAPR and BER of large-scale multiuser MISO SC-FDMA downlink

Recently, large-scale multiuser MISO systems with tens to hundreds of antennas at the base station and one antenna each at the mobiles/user terminals are gaining importance. We evaluated the PAPR and BER performance advantage of SC-FDMA compared to OFDMA in such large systems. We evaluated the BER performance in two systems: $i)$ a system with $n_t = 16, n_r = 1, K = 4, N = 64$, and $ii)$ a system $n_t = 128, n_r = 1, K = 4, N = 64$. In both these systems, $\widetilde{K} = K$ and $M = N$, i.e., each subcarrier can be shared by all users so that for each user is allotted with all N subcarriers. Since $M = N$, there is no distinction between fixed interleaved allocation and dynamic allocation. The PAPR and BER plots in Figs. 7 and 8 show that SC-FDMA is preferred over OFDMA in large-scale multiuser MISO downlink systems as well.

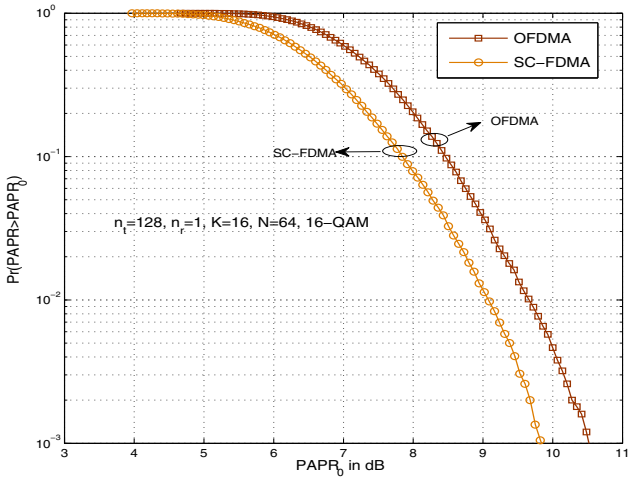

Fig. 7. PAPR performance of large-scale multiuser MISO SC-FDMA and OFDMA for $n_t = 128, n_r = 1, N = 64, K = 16$, 16-QAM.

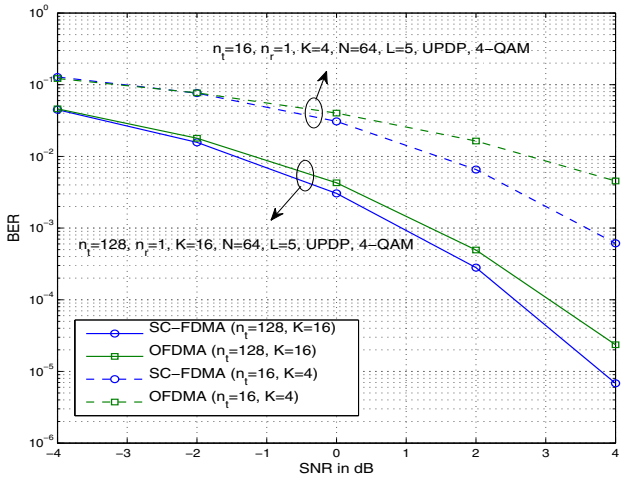

Fig. 8. BER performance of large-scale multiuser MISO downlink SC-FDMA and OFDMA for $i)$ $n_t = 16, n_r = 1, K = 4, L = 5$, 4-QAM, and $ii)$ $n_t = 128, n_r = 1, K = 16, L = 5$, 4-QAM.

In this paper, we have used the LAS algorithm to improve the performance of the FD-MMSE equalizer. Similar low complexity search algorithms like the reactive tabu search (RTS) algorithm [13], [14] can be used in place of the LAS algorithm to further improve performance.

IV. Conclusions

The low PAPR advantage of SC-FDMA over OFDMA has led to the adoption of SC-FDMA on the uplink in wireless standards like LTE. In this paper, we have argued and showed that SC-FDMA can be quite beneficial on the downlink as well. A key advantage is that the transmit power amplifiers in the base station can be operated at more efficient operating points, making the base stations more energy efficient (more 'green'). Also, SC-FDMA retains the desirable feature of flexible allocation of subcarriers in OFDMA because of the DFT-precoded OFDM view of SC-FDMA. To address the equalization requirement at the user terminals in SC-FDMA downlink, we used low complexity equalization algorithms (FD-MMSE equalizer followed by the LAS algorithm) which gave very good performance. We presented simulation results that showed the PAPR and BER performance advantage of SC-FDMA over OFDMA in multiuser SISO/MIMO downlink as well as in large-scale multiuser MISO downlink with tens to hundreds of antennas at the base station. This performance advantage along with the low PAPR advantage makes SC-FDMA a preferred choice for multiuser downlink communication in future wireless systems and standards.

Acknowledgment

This work was supported in part by a gift from The Cisco University Research Program, a corporate advised fund of Silicon Valley Community Foundation.

References

[1] Z. Wang, and G. B. Giannakis, "Wireless multicarrier communications: where Fourier meets Shannon," *IEEE Signal Process. Mag.*, vol. 17, pp. 29-48, May 2000.

[2] H. Sari, G. Karam, and I. Jeanclaude, "Transmission techniques for digital terrestrial TV broadcasting," *IEEE Commun. Mag.*, vol. 33, no. 2, pp. 100-109, February 1995.

[3] D. Falconer, S. L. Ariyavisitakul, A. Benyamin-Seeyar, and B. Eidson, "Frequency domain equalization for single-carrier broadband wireless systems," *IEEE Commun. Mag.,* pp. 58-66, April 2002.

[4] S. Ohno, "Performance of single-carrier block transmissions over multipath fading channels with linear equalization," *IEEE Trans. Signal Process.,* vol. 54, no. 10, pp. 3678-3687, October 2006.

[5] H. G. Myung, J. Lim, and D. J. Goodman, "Single carrier FDMA for uplink wireless transmission," *IEEE Veh. Tech. Mag.,* vol. 1, no. 3, pp. 30-38, September 2006.

[6] H. G. Myung and D. J. Goodman, *Single Carrier FDMA: A New Air Interface for Long Term Evolution*, John Wiley 2008.

[7] K. V. Vardhan, S. K. Mohammed, A. Chockalingam, and B. S. Rajan, "A low-complexity detector for large MIMO systems and multicarrier CDMA systems," *IEEE JSAC Spl. Iss. on Multiuser Detection for Adv. Commun. Sys. and Net.*, vol. 26, no.3, pp. 473-485, April 2008.

[8] S. K. Mohammed, A. Zaki, A. Chockalingam, and B. S. Rajan, "High-rate space-time coded large-MIMO systems: Low-complexity detection and channel estimation," *IEEE Jl. Sel. Topics in Signal Process. (JSTSP): Spl. Iss. on Managing Complexity in Multiuser MIMO Systems*, vol. 3, no. 6, pp. 958-974, December 2009.

[9] W. Liu, L. L. Yang, and L. Hanzo, "SVD assisted joint transmitter and receiver design for the downlink of MIMO system,"*Proc. IEEE VTC'2008*, pp. 1-5, September 2008.

[10] F. Wu and M. A. Abu-Rgheff, "An efficient suboptimal subcarrier allocation algorithm for multiuser OFDM system," *Proc. Int. Conf. on Wireless and Mobile Commn.*, pp. 190-195, August 2009.

[11] T. Ji, C. Zhou, S. Zhou, and Y. Yao, "Low complex user selection strategies for multi-user MIMO downlink scenario," *Proc. IEEE WCNC'2007,* pp. 1534-1539, March 2007.

[12] F. Wu and M. A. Abu-Rgheff, "Efficient subcarrier allocation in downlink multiuser MIMO OFDM systems," *Proc. Int. Symp. on Wireless Commn. Systems (ISWCS)*, pp. 51-55 September 2010.

[13] N. Srinidhi, T. Datta, A. Chockalingam, and B. S. Rajan, "Layered tabu search algorithm for large-MIMO detection and a lower bound on ML performance," *IEEE Trans. Commun.*, vol. 59, no. 11, pp. 2955-2963, November 2011.

[14] N. Srinidhi, S. K. Mohammed, and A. Chockalingam, "A reactive tabu search based equalizer for severely delay-spread UWB MIMO-ISI channels," *Proc. IEEE GLOBECOM'2009*, pp. 1-6, December 2009.